Virologica Sinica 37 (2022) 685–694

Contents lists available at ScienceDirect

Virologica Sinica

journal homepage: www.keaipublishing.com/en/journals/virologica-sinica
www.virosin.org

Research Article

Rottlerin plays an antiviral role at early and late steps of Zika virus infection

Shili Zhou [a,b,1], Quanshi Lin [a,c,1], Changbai Huang [a,c], Xiaotong Luo [a,d], Xu Tian [a,c], Chao Liu [a,d,*], Ping Zhang [a,c,*]

[a] Key Laboratory of Tropical Diseases Control (Sun Yat-sen University), Ministry of Education, Guangzhou, 510080, China
[b] Medical Research Center, Guangdong Second Provincial General Hospital, Guangzhou, 510317, China
[c] Department of Immunology, Zhongshan School of Medicine, Sun Yat-sen University, Guangzhou, 510080, China
[d] Department of Microbiology, Zhongshan School of Medicine, Sun Yat-sen University, Guangzhou, 510080, China

ARTICLE INFO

Keywords:
Zika virus (ZIKV)
Rottlerin
Enveloped virus
Replication

ABSTRACT

Infection of Zika virus (ZIKV) may cause microcephaly and other neurological disorders, while no vaccines and drugs are available. Our study revealed that rottlerin confers a broad antiviral activity against several enveloped viruses, including ZIKV, vesicular stomatitis virus, and herpes simplex virus, but not against two naked viruses (enterovirus 71 and encephalomyocarditis virus). Rottlerin does not have a direct virucidal effect on the virions, and its antiviral effect is independent of its regulation on PKCδ or ATP. Both pretreatment and post-treatment of rottlerin effectively reduce the viral replication of ZIKV. The pretreatment of rottlerin disturbs the endocytosis of enveloped viruses, while the post-treatment of rottlerin acts at a late stage through disturbing the maturation of ZIKV. Importantly, administration of rottlerin in neonatal mice significantly decreased the ZIKV replication *in vivo*, and alleviated the neurological symptoms caused by ZIKV. Our work suggests that rottlerin exerts an antiviral activity at two distinct steps of viral infection, and can be potentially developed as a prophylactic and therapeutic agent.

1. Introduction

Zika virus (ZIKV) belongs to the *Flavivirus* genus of the *Flaviviridae* family, which includes dengue virus (DENV), Japanese encephalitis virus (JEV), and yellow fever virus (YFV) (Musso and Gubler, 2016). ZIKV infection often leads to mild symptoms including fever, rash, or arthralgia (Grant et al., 2016; Lazear and Diamond, 2016; Pierson and Diamond, 2018). However, ZIKV infection in early pregnancy has been also associated with microcephaly of fetus (Schuler-Faccini et al., 2016) and neurological disorders in adults such as Guillain-Barre syndrome (Oehler et al., 2014). Currently, there are no vaccines or specific drugs available.

The genome of ZIKV is a positive single-stranded RNA of 11 kb in length (Wang et al., 2018). Infection of ZIKV begins from attachment to host receptors, leading to an endocytosis (Hamel et al., 2015). Internalized virions fuse with the endosomal membrane, and then its genome RNA is released into the cytoplasm (Stiasny et al., 2011). The viral genome immediately encodes a single polypeptide, which is cleaved by viral and host proteases into ten individual proteins (Kuno and Chang, 2007; Tsetsarkin et al., 2016). Nonstructural proteins induce the rearrangement of membrane compartments of endoplasmic reticulum (ER), forming replication factories (RF). In the RFs, viral RNAs are synthesized and translated into viral proteins (Cortese et al., 2017). Then, progeny virions are assembled and transmitted through the Golgi, during which the immature virions become matured upon prM cleavage by furin (Mukhopadhyay et al., 2005; Pierson and Graham, 2016) and are released.

Rottlerin, a natural polyphenol ketone compound derived from camara powder, is widely used in the function study of PKCδ because of its ability to selectively suppress PKCδ phosphorylation (Mori et al., 2015). Rottlerin confers multiple physiological activities in a PKCδ-independent manner (Maioli et al., 2012). For example, rottlerin inhibits other protein kinases, through blocking the coupling of the mitochondrial respiratory chain and oxidative phosphorylation, and

* Corresponding authors.
E-mail addresses: liuchao9@mail.sysu.edu.cn (C. Liu), zhangp36@mail.sysu.edu.cn (P. Zhang).
[1] Shili Zhou and Quanshi Lin contributed equally to this work.

https://doi.org/10.1016/j.virs.2022.07.012
Received 12 March 2022; Accepted 26 July 2022
Available online 5 August 2022
1995-820X/© 2022 The Authors. Publishing services by Elsevier B.V. on behalf of KeAi Communications Co. Ltd. This is an open access article under the CC BY-NC-ND license (http://creativecommons.org/licenses/by-nc-nd/4.0/).

reducing the ATP production (Maioli et al., 2012). Rottlerin plays multiple roles including anti-oxidation (Maioli et al., 2009), anti-cell proliferation (Torricelli et al., 2008) and angiogenesis (Valacchi et al., 2011), anti-inflammatory (Ishii et al., 2002), and anti-allergic (Daikonya et al., 2002).

Interestingly, rottlerin confers inhibitory activity against many pathogens, including viruses, parasite (Ietta et al., 2017), and bacteria (Pandey et al., 2016; Shivshankar et al., 2008) in cultured cells and in animal models (Kang et al., 2021; Ojha et al., 2021a). The anti-pathogen effect of rottlerin is exerted either through inhibiting the activation of PKCδ, such as human immunodeficiency virus (HIV-1), human T-lymphotropic virus (HTLV-1), Rift valley fever virus (RVFV), and porcine reproductive and respiratory syndrome virus (PRRSV) (Contreras et al., 2012; Filone et al., 2010; Kang et al., 2021; Mori et al., 2015), or through reducing the ATP levels (such as rabies virus) (Lama et al., 2019). Regarding to ZIKV, a recent report showed that rottlerin inhibits its infection in human neuronal stem cells (hNSC) (Ojha et al., 2021b). However, whether the antiviral effect of rottlerin is cell-specific and the exact step that it acts at remains obscure. Our study further revealed that rottlerin inhibited the replication of ZIKV and another two enveloped viruses, but not naked viruses in human lung carcinoma epithelial cells. The anti-ZIKV effect of rottlerin is independent of its regulation on PKCδ or ATP. Intriguingly, rottlerin acts at two different steps of ZIKV infection, one at an internalization step and the other during assembly and egress step. Our data also revealed that rottlerin confers an antiviral activity in an *in vivo* neonatal mouse model.

2. Materials and methods

2.1. Cell culture

Human lung carcinoma epithelial A549 cells (ATCC CCL-185), glioblastoma SNB19 cells (DSMZ ACC-325), human hepatoma Huh7.5 cells (a gift from Dr Yi-Ping Li, Sun Yat-sen University) (Zheng et al., 2021), human embryonic kidney 293T cells (ATCC CRL-3216), and African green monkey kidney Vero cells (ATCC CCL-81) were maintained in Dulbecco Modified Eagle Medium (DMEM) supplemented with 10% fetal bovine serum (FBS) (Gibco, USA) at 37 °C with 5% CO_2. The media were added with 100 units/mL of streptomycin and penicillin (Invitrogen, USA).

2.2. Compounds

Rottlerin (CAS NO 82-08-6), CCCP (CAS NO 555-60-2) were purchased from MedChemExpress, USA. Compounds were dissolved in dimethylsulfoxide (DMSO, Sigma-Aldrich, USA, D2650).

2.3. Antibodies

Primary antibodies included anti-ZIKV E rabbit mAb (Gene Tex, USA, GTX133314), anti-ZIKV C rabbit mAb (Gene Tex, GTX134186), anti-ZIKV prM rabbit mAb (Gene Tex, GTX133305), anti-PKC delta rabbit mAb (Proteintech, USA, 19132-1-AP), anti-β-actin mouse mAb (Sigma, A1978), anti-GAPDH rabbit mAb (Proteintech, 10494-1-AP). Secondary antibodies included IRDye 800 CW conjugated goat anti-rabbit IgG, IRDye 680 RD conjugated goat anti-mouse IgG (LI-COR, USA), horseradish peroxidase-conjugated horse anti-mouse IgG (CST, USA), and goat anti-rabbit IgG (Bio-Rad, USA).

2.4. Cell viability assay

1 mg/mL MTT solution (Genview, USA) was added to cell culture and incubated for 4 h at 37 °C. The supernatant was discarded, and DMSO was added to the plate to dissolve the formazan product. OD value was measured at 490 nm using a BioTek Instrument (BioTek, USA). Cell viability curve was presented as percentage of OD value derived from treated samples to that of the untreated control.

2.5. Plaque assay and focus forming assay (FFA)

In the plaque assay, serial 10-fold dilutions of each sample were prepared, and 100 μL/well of the diluted virus was added into the 12-well plates. The cells were cultured in the mixture of 2× DMEM (Invitrogen) and 2% methylcellulose (Sigma) (v/v 1:1). Visible plaques were counted at 3–4 days post-infection (d.p.i.).

In the FFA, serial 10-fold dilutions of each sample were prepared, and 100 μL/well of diluted virus was added into the 96-well plates. The cells were cultured in the mixture of 2 × DMEM (Invitrogen) and 2% methylcellulose (Sigma) (v/v 1:1). Cells were washed with phosphate-buffered saline (PBS) at 48 h post-infection (d.p.i.), and then fixed with 1% paraformaldehyde (PFA). Cells were incubated with anti-WNV E60 MAb (a gift from Dr Michael S Diamond, Washington University School of Medicine) (Oliphant et al., 2005), followed by incubation with IRDye 680 RD conjugated anti-mouse IgG (LI-COR). The number of spots was determined by ImmunoSpot® S6 Ultra (CTL, USA).

2.6. Detection of virion integrity by sucrose density gradient assay

The media containing 4 × 10^6 PFU ZIKV were mixed with DMSO, DMSO containing 2.5 or 10 μmol/L rottlerin, or 1% (v/v) Triton X-100, respectively, followed by incubation at 37 °C for 2 h. The samples were gently loaded on the top of sucrose gradient with a linear concentration range from 20% to 70%, and then centrifuged in an Optima L-100 XP ultracentrifuge (Beckman Coulter, USA) at 107,170 ×*g* at 4 °C for 3 h. Each gradient was collected in eight fractions. The ZIKV RNA and E protein levels in each fraction were detected by real-time PCR and Western blot, respectively (Yu et al., 2017).

2.7. Generation of wild-type PKCδ ($PKC\delta^{WT}$)- and constitutively active PKCδ ($PKC\delta^{CAT}$)-expressing cells

cDNAs prepared from A549 cells were used as a PCR template. Full-length or constitutively active truncated fragments of the *PRKCD* gene were amplified by PCR and inserted into the lentiviral vector CSII-EF-MCS-IRES2-Venus. The sequences of primers used were shown in Supplementary Table S1. 293T cells were transfected with CSII-PKCδ^{WT} or CSII-PKCδ^{CAT}, psPAX2, and pMD2.G using FuGENE® HD Transfection Reagent (Promega, USA). Supernatants were collected at 2 days post-transfection and passed through a 0.45-μm filter. Then A549 cells were incubated with the supernatants containing lentiviruses CSII-PKCδ$^{WT/CAT}$. The PKCδ^{WT}- and PKCδ^{CAT}-expressing A549 cells were sorted by flow cytometry and confirmed by Western blot.

2.8. RNA interference

The siRNA with scrambled sequence was used as negative control (siNC). Sequence of siRNA targeting human PKCδ RNA (siPKCδ) was 5′-CGACAAGAUCAUCGGCAGATT-3′. The siRNAs were synthesized commercially by RiboBio and transfected into A549 cells using Lipofectamine 2000 (Invitrogen) according to the manufacturer's instruction. Cells were harvested or applied for further assay at 48 h post-transfection.

2.9. Western blot

Cells were lysed in RIPA lysis buffer (pH 7.4) [50 mmol/L Tris-HCl, 0.5% (v/v) NP-40, 1% Triton-100, 150 mmol/L NaCl, 1 mmol/L EDTA, 1 mmol/L phenylmethanesulfonyl fluoride (PMSF), 1% protease inhibitor cocktails (PIC), 1 mmol/L sodium orthovanadate (Na_3VO_4), and 1 mmol/L sodium fluoride (NaF)]. Proteins were separated on SDS-PAGE and transferred onto nitrocellulose membranes. Then membranes were

blocked in 0.1% PBST with 5% bovine serum albumin (BSA) (New England Biolabs, USA), and incubated with primary antibodies at 4 °C overnight. After washed by 1 × TBST for three times, the membranes were incubated with IRDye 800 CW-conjugated anti-rabbit IgG and IRDye 680 CW-conjugated anti-mouse IgG secondary antibody (LI-COR) according to the manufacturer's protocols. Fluorescent bands were visualized using the Odyssey infrared imaging system (LI-COR) as described previously (Zhou et al., 2019).

2.10. Quantitative real-time (qRT) PCR

Total cellular RNA was extracted using TRIzol reagent (Invitrogen) and reverse-transcribed using HiScript® II Q RT SuperMix (Vazyme, China) according to the manufacturer's protocol. Sequences of qRT-PCR primers were listed in Supplementary Table S2. The qRT-PCR was performed with LightCycler 480 SYBR Green I Master (Roche) in a CFX96 Real-Time System (Bio-Rad). Relative RNA level was normalized to β-actin and calculated by $2^{-\Delta\Delta Ct}$ methods as described previously (Zhou et al., 2019).

2.11. Measurement of intracellular ATP level

Intracellular ATP levels were measured using the ATP Assay Kit (S0026, Beyotime Biotechnology, China) according to the manufacturer's instructions.

2.12. Time of addition assay

A549 cells were infected with ZIKV at an MOI of 3 for 1 h. Infected cells were treated with 2.5 μmol/L rottlerin at 1 h prior to infection or at 0, 1, 6, 12, 18 h.p.i. At 24 h p.i., supernatants were collected for focus forming assay.

2.13. Viral attachment and internalization assay

A549 cells were incubated in control (DMSO) or rottlerin from 2 h before virus infection to the end of experiment. Cells were infected with ZIKV, vesicular stomatitis virus (VSV) or herpes simplex virus (HSV) at an MOI of 3 at 4 °C for 1 h, and were then washed by PBS for three times. Cells were harvested for RNA extraction and qRT-PCR to detect the RNA level of virions binding to the cell membrane. For internalization assay, cells were infected with ZIKV, VSV or HSV (MOI = 3) at 4 °C for 1 h and then cultured in DMEM containing NH_4Cl at 37 °C for 0.5 h. The media were removed and cells were treated by ice-cold proteinase K for 45 min, and were then washed by PBS for three times. Cells were harvested for RNA extraction and qRT-PCR to detect the RNA level of virions internalized into cells.

2.14. Transmission electron microscopy

A549 cells were infected with mock or ZIKV at an MOI of 3, followed by DMSO or rottlerin treatment at 1 h.p.i. Cells were collected at 24 h.p.i. and fixed by 2.5% glutaraldehyde after PBS wash. The cells were post-fixed in 1% osmium tetroxide and embedded in Araldite resin. Blocks were sectioned with a diamond knife on an ultramicrotome and examined with a transmission electron microscope (Tecnai G2 Spirit Twin, FEI, USA).

2.15. Animal experiments

Pregnant Kunming mice were purchased and maintained under specific-pathogen-free conditions at the animal facility of Sun Yat-sen University. Neonatal Kunming mice were breastfed by their mothers and divided into different groups. Two-day-old neonatal Kunming mice were treated with DMSO or rottlerin (6 mg/kg of body weight) in a 20 μL volume by intracerebral injection. After 1 h, mice were intracerebrally inoculated with PBS or ZIKV suspension (4×10^4 PFU) in a 20 μL volume and monitored over 14 days. All animals were cage-bred with the mouse mothers during the experiment and observed daily until the development of symptoms. All mice were euthanized by cervical dislocation after the appearance of severe clinical signs, including lethargy and paralysis. Whole-brain tissue homogenates were prepared using an automated homogenizer. Tissues were ground with PBS buffer and centrifuged at 12,000 ×*g* for 15 min at 4 °C. The supernatants were collected and stored at −80 °C for later use. Total RNA was extracted using TRIzol reagent (Invitrogen) according to the manufacturer's instructions to detect the viral RNA copies. The supernatants from neonatal mouse brains were filtered through 0.45 μm filter, and plaque assay was performed to detect the titers of ZIKV.

2.16. Statistical analysis

All statistical analyses were performed with an unpaired, two-tailed Student's *t*-test using GraphPad Prism software (verison 7.0). Data were presented as mean ± standard deviation from at least three independent experiments. The differences were considered statistically significant when $P < 0.05$.

3. Results

3.1. Rottlerin confers an antiviral activity against enveloped viruses

To test the toxicity of rottlerin, A549 cells were treated with different doses of rottlerin for 24 h and cell viability was measured by MTT assay. The 50% cellular cytotoxicity (CC_{50}) of rottlerin in A549 was 47.78 μmol/L (Fig. 1A), indicating that rottlerin did not have a significant toxicity to cells. Then, A549 cells were infected with ZIKV, followed by rottlerin treatment ranging from 0 to 5 μmol/L. At 24 h.p.i., supernatants were harvested for plaque assay. Rottlerin displayed a dose-dependent inhibitory effect on ZIKV yields, and the 50% inhibitory concentration (IC_{50}) was 1.06 μmol/L (Fig. 1B). As 2.5 μmol/L rottlerin led to more than 90% inhibition of ZIKV yield, we chose this concentration in the following assays unless indicated. Next, we tested the effect of rottlerin on ZIKV replication in another two human cell lines, SNB19 and Huh7.5 cells. The data showed that the IC_{50} of rottlerin against ZIKV in SNB19 cells and Huh7.5 cells were 0.19 μmol/L and 0.70 μmol/L, respectively (Fig. 1C and D), demonstrating that the antiviral effect of rottlerin was not cell-specific.

In addition, we tested the role of rottlerin in the replication of another two enveloped viruses, VSV and HSV, and two naked viruses, enterovirus 71 (EV71) and encephalomyocarditis virus (EMCV). Interestingly, rottlerin posed a dose-dependent inhibitory effect on both VSV and HSV (Fig. 1E), but not on the naked viruses (EV71 and EMCV) (Fig. 1F), suggesting that rottlerin might interfere with a common step in replication of enveloped viruses.

3.2. Rottlerin does not destroy the integrity of ZIKV envelope

As antiviral compounds possibly pose a destructive effect on the structure of viral envelope, we investigated the impact of rottlerin on the integrity of ZIKV by sucrose density gradient assay. Media containing ZIKV virions were treated with 1% (v/v) DMSO (control), 2.5 or 10 μmol/L rottlerin, or 1% (v/v) Triton X-100 as a positive control, followed by incubation at 37 °C for 2 h. The samples in the sucrose gradients were centrifuged and then fractionated into eight fractions. The viral RNA and protein levels in each fraction were detected by qRT-PCR and Western blot. As shown in Fig. 2, the ZIKV RNA and E protein of the DMSO-treated sample were both detected in the fractions 5 and 6, indicating that the virions were intact. In contrast, the viral RNAs and proteins in the Triton X-100-treated sample were allocated to different fractions. Viral RNAs were mainly detected in fractions 5–8, while E proteins were located in fractions 1–4, indicating that virion structure

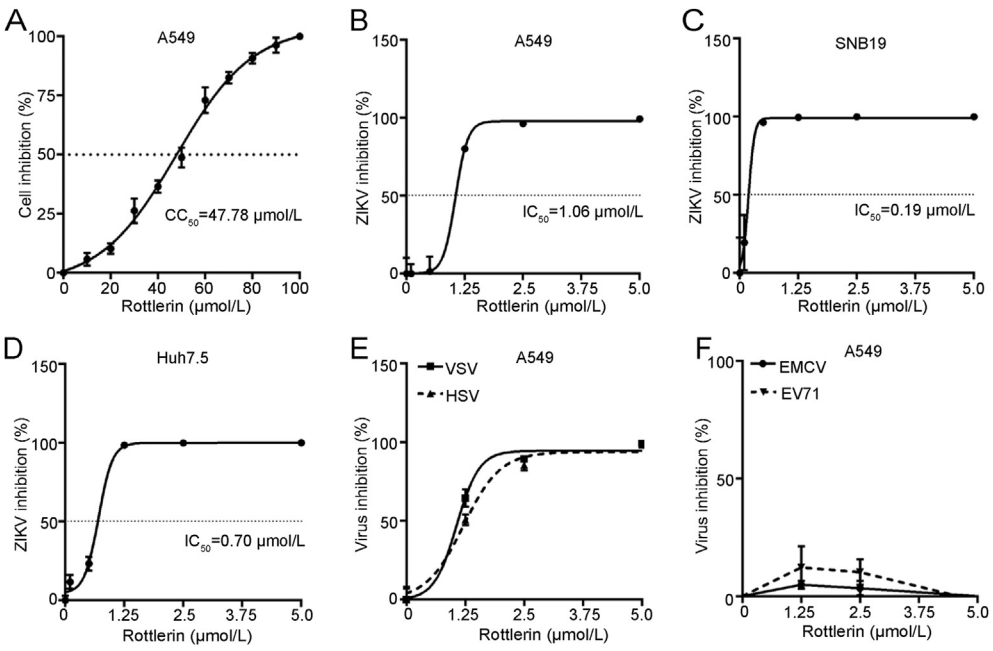

Fig. 1. Rottlerin inhibits the replication of ZIKV. **A** A549 cells were treated with rottlerin at indicated concentrations for 24 h. Cell viability was measured by MTT assay. **B–D** A549, SNB19, or Huh7.5 cells were infected with ZIKV (MOI = 3), followed by rottlerin treatment from 1 h.p.i. to the end of assay. At 24 h.p.i., supernatants were collected for plaque assay or FFA. **E, F** A549 cells were infected with VSV, HSV, EMCV, or EV71, followed by rottlerin treatment from 1 h.p.i. to the end of assay. At 24 h.p.i., supernatants were collected for plaque assay or FFA. Data are shown as mean ± standard deviation of at least three independent experiments. FFA, focus forming assay; ZIKV, Zika virus; VSV, vesicular stomatitis virus; HSV, herpes simplex virus; EMCV, encephalomyocarditis virus; EV71, enterovirus 71; h.p.i., hours post infection; CC_{50}, 50% cytotoxic concentration; IC_{50}, 50% inhibition concentration.

was disrupted. The viral RNAs and proteins of the rottlerin-treated viruses were similar to that of the DMSO-treated group, mostly detected in fractions 5 and 6, indicating that the integrity of virions was not affected by rottlerin treatment.

3.3. The antiviral effect of rottlerin is independent of PKCδ or ATP

As rottlerin has been widely used as an inhibitor of PKCδ (Maioli et al., 2012), we assessed whether the antiviral effect of rottlerin

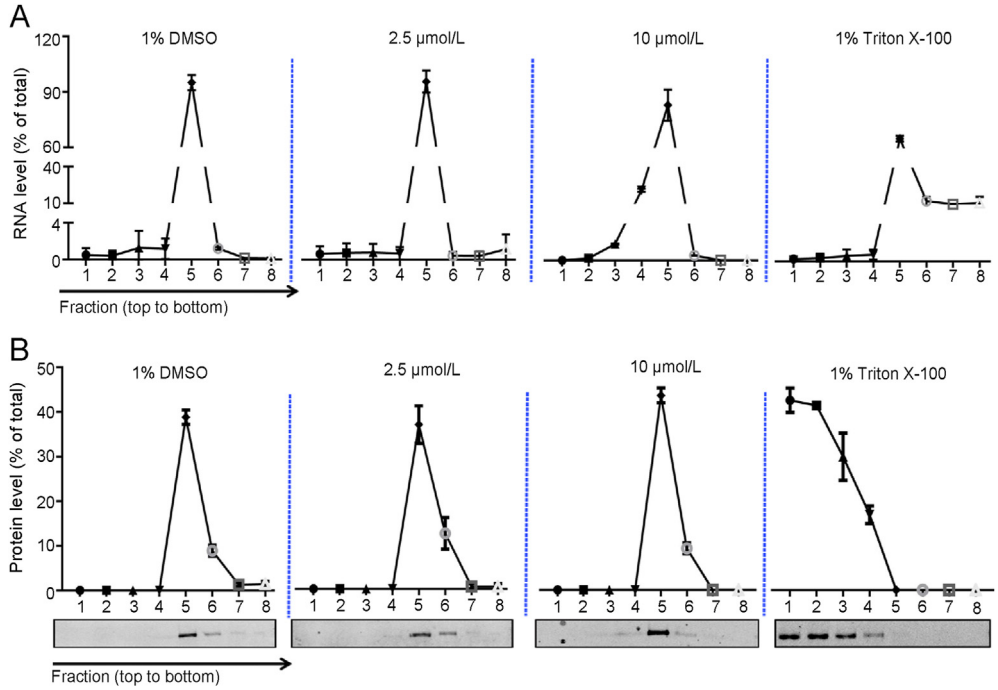

Fig. 2. Rottlerin does not destroy the virion integrity of ZIKV. **A, B** ZIKV virions were treated with DMSO, rottlerin (2.5 or 10 μmol/L), or Triton X-100, followed by sucrose gradient centrifugation. Viral RNAs in each fraction were detected by real-time PCR (**A**). Percentages of total E protein was measured by Western blot and analyzed by Image J (**B**). Data are shown as mean ± standard deviation of at least three independent experiments.

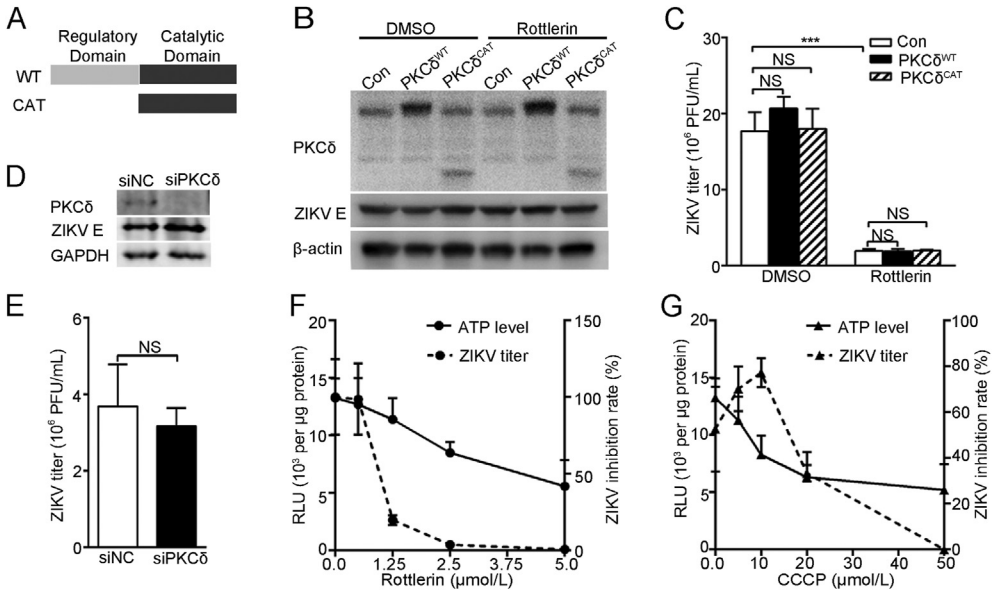

Fig. 3. The antiviral effect of rottlerin is independent of its inhibition on PKCδ or ATP. **A–E** Role of PKCδ in ZIKV infection. Control, PKCδ^{WT}- or PKCδ^{CAT}-expressing A549 cells were infected with ZIKV (MOI = 3), followed by DMSO or rottlerin-treatment from 1 h.p.i. Cells and supernatants were collected at 24 h.p.i. for Western blot (**B**) and plaque assay (**C**). **D, E** RNAi assay. A549 cells were transfected with siNC or siPKCδ for 48 h, followed by ZIKV infection at an MOI of 3. Cells were harvested at 24 h.p.i. for Western blot (**D**) and plaque assay (**E**). **F, G** Effect of rottlerin on ATP levels and viral titers. CCCP was probed as a positive control. For ATP level measurement, A549 cells were treated with indicated concentrations of rottlerin (**F**) or CCCP (**G**), and harvested at 24 h. For viral titer determination, A549 cells were infected with ZIKV (MOI = 3), followed by treatment of rottlerin (**F**) or CCCP (**G**) from 1 h.p.i. Supernatants were harvested at 24 h.p.i. for FFA. Data are shown as mean ± standard deviation of at least three independent experiments. Statistical analysis was performed with an unpaired, two-tailed Student's *t*-test using GraphPad Prism software. ***$P < 0.001$. NS, not significant; CAT, constitutively active; h.p.i., hours post-infection.

depended on its inhibition of PKCδ activation. We generated stable PKCδ^{WT}- or PKCδ^{CAT}-expressing A549 cells (Fig. 3A). Control cells, PKCδ^{WT}, and PKCδ^{CAT} cells were infected with ZIKV, followed by DMSO or rottlerin-treatment from 1 h.p.i. to the end of assay. Expression of PKCδ^{WT} or PKCδ^{CAT} did not alter the viral E protein levels (Fig. 3B) and viral yields (Fig. 3C), regardless the absence or presence of rottlerin. To further validate the role of PKCδ in the ZIKV replication, we silenced PKCδ through an RNAi strategy. Cells were transfected with siNC or siPKCδ, followed by ZIKV infection at 48 h.p.i. The cells and supernatants were harvested for Western blot or plaque assay. The level of PKCδ in the

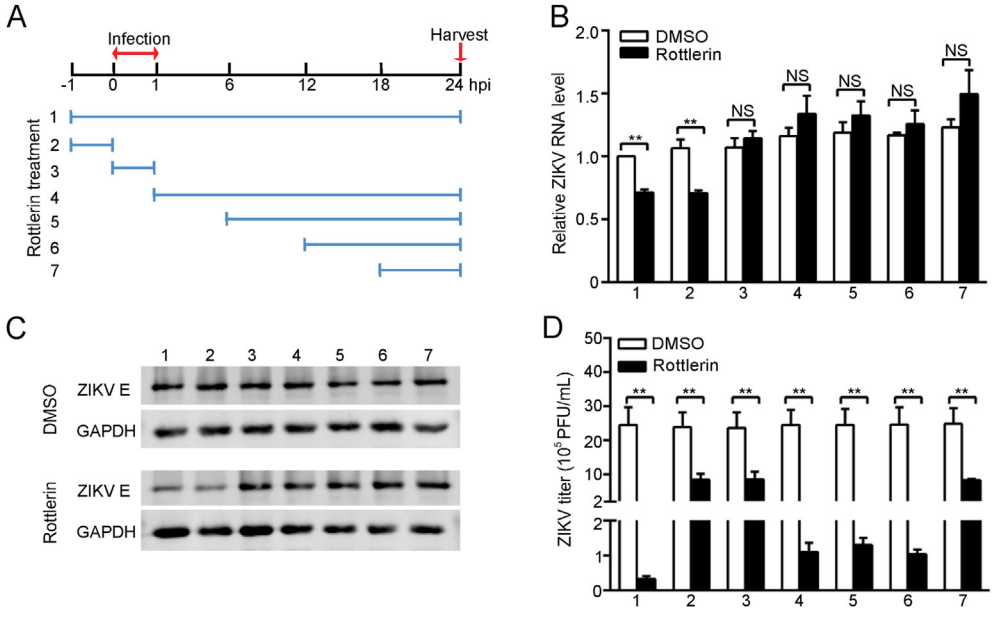

Fig. 4. Time-of-addition assay of rottlerin against ZIKV infection. **A** A549 cells were infected with ZIKV (MOI = 3), rottlerin was applied to cells during indicated time frames. Cells were harvested at 24 h.p.i. for viral RNA detection (**B**) or Western blot (**C**), and supernatants were collected for FFA (**D**). Relative RNA level was normalized to β-actin and calculated by $2^{-\Delta\Delta Ct}$ methods. Data are shown as mean ± standard deviation of at least three independent experiments. Statistical analysis was performed by unpaired two-tailed Student's *t*-test. **$P < 0.01$. NS, not statistically significant; FFA, focus forming assay.

siPKCδ-transfected cells was significantly lower than in the siNC-transfected cells (Fig. 3D), validating that the knockdown of PKCδ was effective. As expected, the PKCδ knockdown did not alter the ZIKV E protein level and viral yields (Fig. 3D and E), suggesting that PKCδ was not required for ZIKV replication.

Apart from inhibiting PKCδ, rottlerin also reduces the ATP production (Lama et al., 2019). To test whether rottlerin inhibits viral infection through down-regulating the ATP level, we compared the cellular ATP levels in the absence and presence of rottlerin. A549 cells were treated with DMSO, rottlerin, or CCCP, a mitochondrial uncoupler as the positive control (Tapia et al., 2006). Both rottlerin and CCCP showed a dose-dependent inhibitory effect on the cellular ATP levels and viral yields of ZIKV (Fig. 3F and G), suggesting that ATP reduction might be correlated with the ZIKV replication. To be noted, at low doses (2.5 μmol/L or below), rottlerin did not significantly reduce the ATP levels, but still inhibited the viral infection, suggesting that the antiviral activity of rottlerin at low doses does not rely on its inhibition on ATP.

3.4. Rottlerin inhibits two different steps of ZIKV replication

To determine which step of ZIKV infection is blocked by rottlerin, we performed a time-of-addition assay. Rottlerin was applied to the cells throughout the whole infection process (group 1), pre- (group 2, 1 h prior to infection), during- (group 3), or post- (1, 6, 12, 18 h.p.i., group 4, 5, 6, 7 respectively) infection (Fig. 4A). As a control, DMSO treatment had no significant effect on viral RNA levels (white bars, Fig. 4B), E protein levels (Fig. 4C), and viral titers (white bars, Fig. 4D). Treatment of rottlerin throughout the infection showed a pronounced reduction of viral RNA levels, protein levels, and titers (group 1, Fig. 4B–D). Pretreatment of rottlerin (group 2) led to a similar reduction of viral RNA and protein as group 1, while the viral titer was only downregulated by around 2.8-fold. Treatment of rottlerin during incubation (group 3) barely affected viral replication levels. Surprisingly, although the viral RNA or protein levels in the post-treatment groups (group 4–7) were barely inhibited by rottlerin, the viral titers were significantly reduced, especially when drug was applied at 1–12 h.p.i. (group 4–6). These observations indicated that rottlerin acts at different steps: its pretreatment might disturb an early step, while its post-treatment might disturb the assembly or egress step.

3.5. Rottlerin inhibits the internalization of three enveloped viruses

As pretreatment of rottlerin was sufficient to reduce the viral RNA level, we proposed that rottlerin might disturb the viral entry. To test this hypothesis, we first examined role of rottlerin in the entry of three enveloped viruses, including ZIKV, VSV, and HSV. A549 cells were pre-treated with DMSO or rottlerin, followed by virus inoculation. Cells were

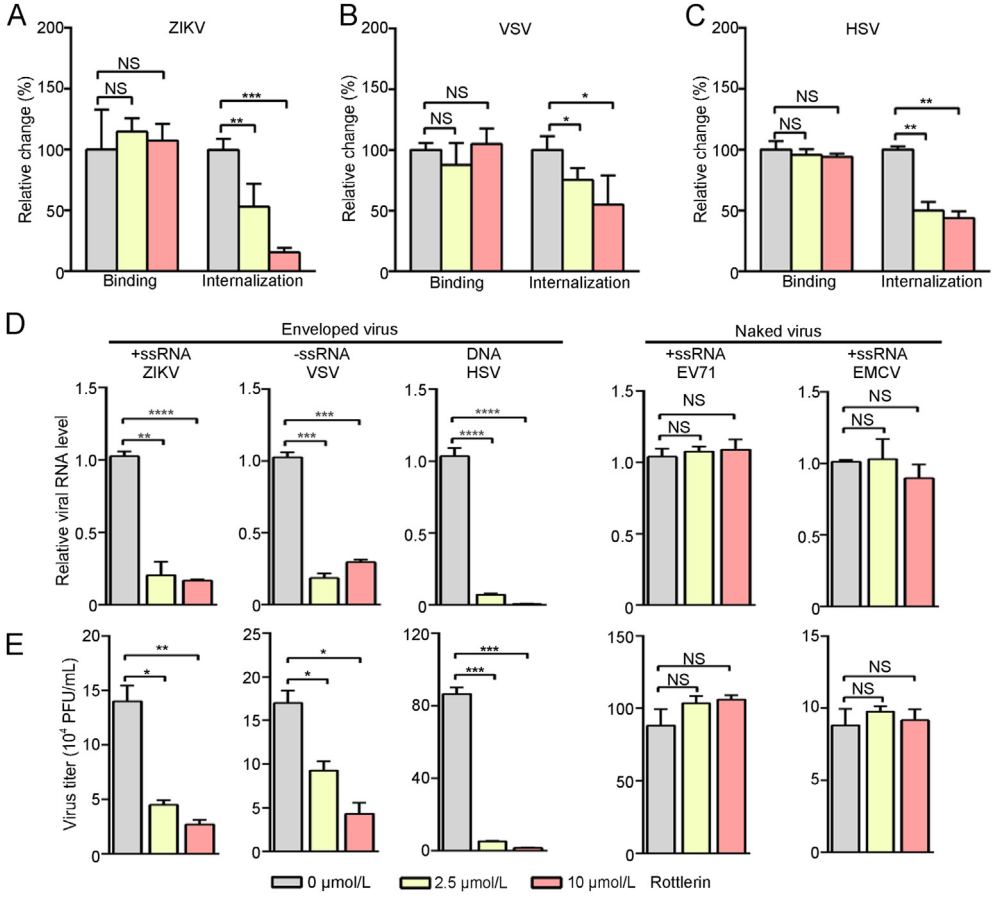

Fig. 5. Pretreatment of rottlerin impairs the entry of enveloped viruses. **A–C** Effect of rottlerin pretreatment on viral binding and internalization. A549 cells were pretreated with DMSO or rottlerin, followed by infection of ZIKV, VSV or HSV (MOI = 1) at 4 °C for 1 h. Cells were harvested for RNA extraction and qRT-PCR to detect the amount of viral particles binding to cell surface. Or cells were further incubated at 37 °C for 0.5 h, and then were harvested for qRT-PCR to detect the level of internalized viral particles. **D, E** Effect of rottlerin pretreatment on viral replication. A549 cells were pretreated with rottlerin for 1 h, followed by viral infection (ZIKV, VSV, HSV, EV71, and EMCV) at MOI 1 for 1 h. At 24 h.p.i., total RNAs were extracted for qRT-PCR (**D**), and supernatants were collected for plaque assay (**E**). Relative change was normalized to negative control, and relative RNA level was normalized to β-actin and calculated by $2^{-\Delta\Delta Ct}$ methods. Data are shown as mean ± standard deviation of at least three independent experiments. Statistical analysis was performed by unpaired two-tailed Student's *t*-test. $^{*}P < 0.05$, $^{**}P < 0.01$, $^{***}P < 0.001$. NS, not statistically significant; ZIKV, Zika virus; VSV, vesicular stomatitis virus; HSV, herpes simplex virus; h.p.i., hours post infection.

incubated at 4 °C for 1 h. The viral RNA levels in the DMSO or rottlerin-treated cells were comparable, indicating that rottlerin did not affect the attachment of these viruses (Fig. 5A–C). Then, we tested effect of rottlerin on the viral endocytosis. The cells were pretreated with DMSO or rottlerin, followed by virus infection. Treatment of 2.5 μmol/L and 10 μmol/L rottlerin led to significant reductions of internalized viral RNA levels in a dose-dependent manner, suggesting that rottlerin interfered with viral endocytosis step of these enveloped viruses (Fig. 5A–C).

Next, we measured the effect of rottlerin pretreatment in the replication of enveloped viruses (VSV and HSV) and naked viruses (EV71 and EMCV). Pretreatment of rottlerin alone dramatically downregulated the viral RNA levels and yields of all three enveloped viruses (ZIKV, VSV, and HSV), but not of two naked viruses (EV71 and EMCV) (Fig. 5D and E). These data indicated that pretreatment of rottlerin specifically affected the entry of enveloped viruses.

3.6. Rottlerin interferes with release of infectious particles of ZIKV

Next, we probed the mechanism that how post-treatment of rottlerin inhibited the ZIKV infection. A549 cells were infected with ZIKV, followed by rottlerin treatment from 1 h.p.i. to the end of assay. Cells and supernatants were collected at indicated time points for qRT-PCR, Western blot, or transmission electron microscopy. The viral RNA and E protein levels were comparable between rottlerin- and DMSO-treated groups at each time point (Fig. 6A and B). Under the transmission electron microscopy, rottlerin treatment alone did not alter the morphological structure of cell organelles (the second panel, Fig. 6C). In both DMSO and rottlerin-treated cells, the morphological changes triggered by ZIKV infection were similar. The endoplasmic reticulum (ER) membrane showed apparent proliferation, dilation, and remodeling, and virions were visualized in the ER lumen (Fig. 6C). These data suggested that post-treatment of rottlerin did not affect the viral RNA replication and translation.

Then, we compared whether post-treatment of rottlerin affected the amounts of non-infectious and infectious virions by measuring the extracellular viral RNA levels in the supernatants. At all tested time points (6, 9, 12, 18, and 24 h.p.i.), the viral RNA levels of rottlerin- and DMSO-treated cells were comparable (Fig. 6D). Similarly, the viral E and C protein levels in the DMSO or drug-treated supernatants were similar, indicating that the amounts of virions released into supernatant were not affected by rottlerin. Intriguingly, the protein level of prM, an indicator of immature virion in the rottlerin-treated group was significantly higher than that in the mock-treated group (Fig. 6E), suggesting that rottlerin might interfere with the maturation process of the virions. The post-treatment of rottlerin did not affect the extracellular RNA levels of VSV, HSV, EV71 or EMCV as well (Fig. 6F). In contrast, rottlerin dramatically reduced the titers of ZIKV, VSV, and HSV, but not of the two naked viruses (Fig. 6G and H). These data indicated that rottlerin might disturb the maturation process of enveloped viruses.

3.7. Rottlerin blocks ZIKV replication in vivo

To test whether rottlerin has an antiviral effect *in vivo*, we chose Kunming neonatal mice as a ZIKV infection model. Kunming neonatal

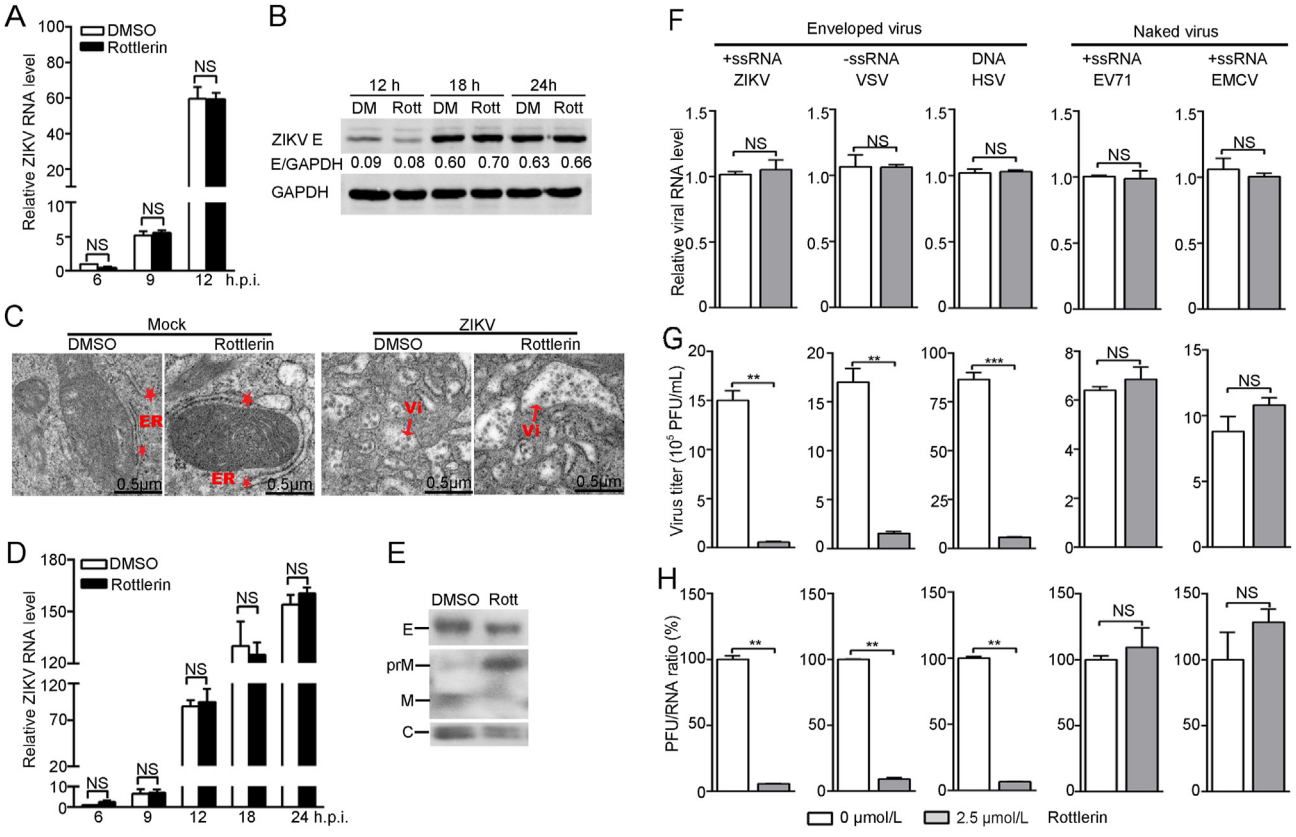

Fig. 6. Post-treatment of rottlerin interferes with PrM cleavage. **A–E** A549 cells were infected with ZIKV (MOI = 3) for 1 h, followed by rottlerin treatment from 1 h.p.i. Cells were harvested at indicated time for qRT-PCR (**A**) or Western blot (**B**). Subcellular structures were visualized by transmission electron microscopy. Asterisk indicates endoplasmic reticulum (ER). Arrow indicates virions (vi) (**C**). Virus particles in the supernatants were collected by ultracentrifugation. Viral RNA and protein levels were detected by qRT-PCR at indicated time (**D**) or Western blot at 24 h.p.i. (**E**). **F, G** A549 cells were infected with ZIKV, VSV, HSV, EMCV, or EV71 at MOI 1 for 1 h, followed by rottlerin treatment from 1 h.p.i. Supernatants were harvested at 24 h.p.i. for qRT-PCR (**F**) or plaque assay (**G**), and PFU/genomic RNA ratio was calculated (**H**). Relative RNA level was normalized to β-actin and calculated by $2^{-\Delta\Delta Ct}$ methods. Data are shown as mean ± standard deviation of at least three independent experiments. Statistical analysis was performed by unpaired two-tailed Student's *t*-test. $^*P < 0.05$, $^{**}P < 0.01$, $^{***}P < 0.001$.

mice were intracerebrally injected with DMSO or 6 mg/kg rottlerin, followed by inoculation with PBS or ZIKV (4×10^4 PFU). The body weights and percentages of survival were monitored daily after infection. The mouse brains were collected at 10 d.p.i. for detection of viral replication levels. At 14 d.p.i., all the DMSO-treated mice died while 75% of the rottlerin-treated mice survived (Fig. 7A). The growth of DMSO-treated mice was gradually retarded from 7 d.p.i., which was significantly alleviated by rottlerin treatment (Fig. 7B). At 10 d.p.i., the DMSO-treated mice exhibited severe neurological symptoms, including tremor, ataxia, and hind limb paralysis. The rottlerin treatment reduced the weight loss and severity of hind limb paralysis caused by ZIKV infection (Fig. 7C).

As expected, the viral RNA copies and viral loads in the brains of rottlerin-treated mice were dramatically lower than the control mice (Fig. 7D and E). These data indicated that rottlerin provided an effective protection against ZIKV-caused diseases *in vivo*.

4. Discussion

ZIKV has become a public health emergency due to its rapidly spread and its association with severe congenital defects. Current study revealed that a natural compound, rottlerin, protected host cells from the infection of three enveloped viruses including ZIKV in A549 cells. Several findings have emerged from our study.

First, we showed that rottlerin is safe within its effective dosage. In A549 cells, the CC_{50} is 47.78 μmol/L, while it effectively inhibits the ZIKV replication at 2.5 μmol/L. This finding is consistent with other reports (Ojha et al., 2021a), and is also supported by a fact that rottlerin has been used as an herb in India, treating a variety of diseases including kapha and bleeding disorders, infection of worms, and abdominal tumors, etc. The reduction of cell viability caused by high dose rottlerin might be due to reduced ATP level or PKC activity.

In a latest publication, Ohja et al. reported that rottlerin inhibited the infection of ZIKV in hNSCs (Ojha et al., 2021b). We further confirmed that rottlerin inhibited the replication of ZIKV and another two enveloped viruses (VSV and HSV) in the human lung carcinoma epithelial cells A549. To date, rottlerin has been documented to inhibit the infection of many enveloped viruses, including HIV-1 (Contreras et al., 2012), HTLV-1 (Mori et al., 2015), Rift valley fever virus (Filone et al., 2010), PRRSV (Kang et al., 2021), rabies virus (Lama et al., 2019), La Crosse virus (Ojha et al., 2021a), SARS-CoV-2 (Chen et al., 2021), chikungunya virus (Abdelnabi et al., 2017). This study further revealed that rottlerin conferred an antiviral activity against ZIKV and dengue virus (Supplementary Fig. S1) in different cells, strengthening its possibility to clinical application.

Based on the observations that rottlerin pretreatment leads to significant reduction of viral replication in a time-of-addition assay (Fig. 4, group 1), and blocks the internalized virion levels (Fig. 5A), we deduce that pretreatment of rottlerin acts at the endocytosis step of ZIKV. Our conclusion was contradictory with the observations reported in hNSCs cells, in which the pretreatment or co-treatment did not affect the viral replication (Ojha et al., 2021b). This discrepancy could be due to different cells tested: ZIKV probably utilizes an alternative route which A549 epithelial cells lack to enter hNSCs. The redundancy of ZIKV entry routes in neuron cells might contribute to its neurotropic feature. Nevertheless, rottlerin also affects the macropinocytosis of Kaposi's sarcoma-associated herpes virus (Raghu et al., 2009) and vaccinia virus (Sandgren et al., 2010), or internalization of PRRSVs. As enveloped viruses shared a common entry mechanism, rottlerin possibly blocks a common entry route of enveloped viruses.

The post-treatment of rottlerin also confers an antiviral activity. The addition of rottlerin as late as 12 h.p.i. efficiently decreased the infectious virion amount, while the viral RNA and protein levels were not affected, indicating that the drug disturbed a very late stage of viral replication. This finding was further confirmed by following observations: (1) the post-treatment of rottlerin reduced the amount of infectious virions (virus titer) (Fig. 6D), but not the viral RNA and protein levels (Fig. 6A and B); (2) the rottlerin-treatment impaired the prM-M protein cleavage

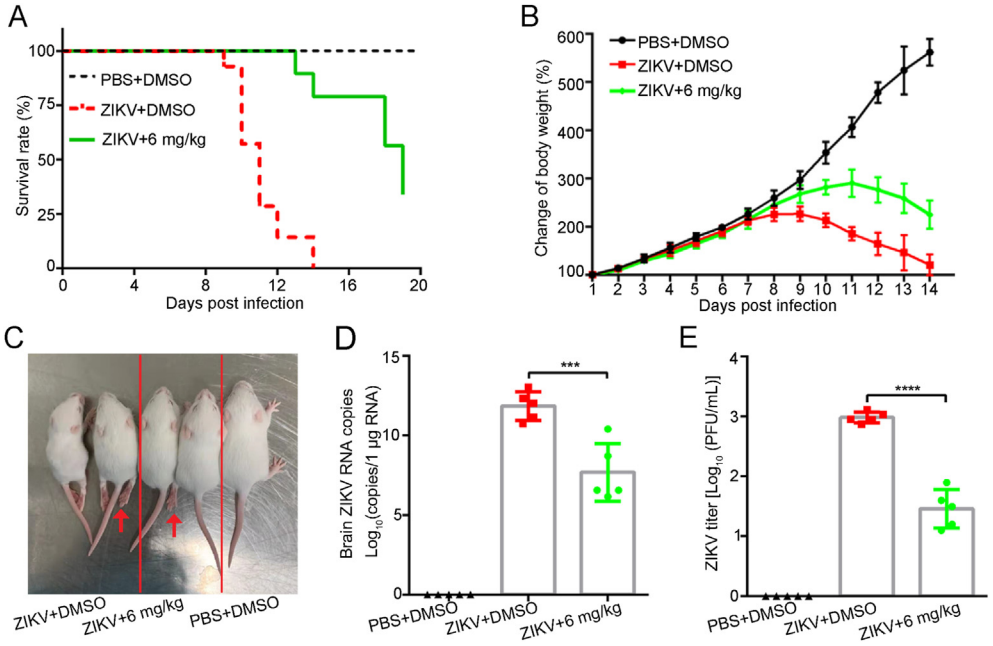

Fig. 7. Rottlerin suppresses the ZIKV replication in the Kunming neonatal mice. Kunming neonatal mice were treated with DMSO or 6 mg/kg rottlerin by intracerebral injection, followed by inoculation with PBS or ZIKV (4×10^4 PFU) at 1 h later. **A** Survival curves of neonatal mice under different treatment conditions (n = 5). **B** Mouse body weight was monitored daily (n = 5). Error bars indicate standard errors of the means. **C** Representative images of neonatal mice under different treatment conditions. Red arrows indicated hind limb paralysis. **D, E** ZIKV replication levels in mouse brains. The brains of neonatal mice were isolated at 10 d.p.i. for detection of viral replication levels (n = 5). Viral RNA copies (**D**) and titers (**E**) were determined by qRT-PCR and plaque assay, respectively. Viral RNA copies were expressed as viral RNA equivalents per microgram upon comparing with a standard curve produced by gradient 10-fold dilutions of ZIKV RNA. Data are shown as mean ± standard deviation of at least three independent experiments. Statistical analysis was performed by unpaired two-tailed Student's *t*-test. *** $P < 0.001$, **** $P < 0.0001$.

of virions (Fig. 6E), implying that rottlerin disturbed the maturation step of ZIKV. As rottlerin inhibits chlamydia from extracting sphingomyelin, which is an important component of viral envelope, rottlerin might reduce the stability of virus envelope, and hence decrease the infectivity of progeny virions. Similarly, Ojha et al. reported that rottlerin disturbed the viral infection upon entry in hNSCs (Ojha et al., 2021b), although they did not further probe which step rottlerin acted at. Our data indicated that low dose of rottlerin reduces the ZIKV infection independent of its inhibition on PKCδ or ATP, which is different from its action against HIV-1 and rabies virus (Contreras et al., 2012; Lama et al., 2019). The precise mechanism of rottlerin against ZIKV infection remains to be further elucidated.

5. Conclusions

In summary, our work reveals that rottlerin acts at an early entry step and a post-translational step in a PKCδ-independent way. Moreover, rottlerin confers a broad protective activity against three enveloped viruses including ZIKV, HSV, and VSV. Therefore, rottlerin could serve as a potent agent applied in both prophylactic and therapeutic treatment against virus infection.

Data availability

All data related to this study are included in the article or uploaded as supplementary information. Other data can be obtained from the corresponding author if reasonably required.

Ethics statement

All the animal experiments were approved by the Institutional Animal Care and Use Committee of Sun Yat-sen University, Guangzhou, China (ethics reference number: 2020–000211).

Author contributions

Shili Zhou: methodology, investigation, data curation, writing-original draft. Quanshi Lin: methodology, investigation, validation, data curation. Changbai Huang: investigation, visualization. Xiaotong Luo: investigation, formal analysis. Xu Tian: validation, formal analysis. Chao Liu: supervision, writing-reviewing, editing, funding acquisition. Ping Zhang: supervision, project administration, writing-reviewing and editing, funding acquisition.

Conflict of interest

The authors declare that they have no known competing financial interests or personal relationships that could have appeared to influence the work reported in this paper.

Acknowledgements

This work was supported by Guangzhou Municipal Science and Technology Program (202206010114), National Natural Science Foundation of China (31970887, 92169110), Doctoral workstation foundation of Guangdong Second Provincial General hospital (2020BSGZ036), and Natural Science Foundation of Guangdong Province (2021A1515011491, 2022A1515010451).

Appendix A. Supplementary data

Supplementary data to this article can be found online at https://doi.org/10.1016/j.virs.2022.07.012.

References

Abdelnabi, R., Amrun, S.N., Ng, L.F., Leyssen, P., Neyts, J., Delang, L., 2017. Protein kinases C as potential host targets for the inhibition of chikungunya virus replication. Antivir. Res. 139, 79–87.
Chen, F., Shi, Q., Pei, F., Vogt, A., Porritt, R.A., Garcia Jr., G., Gomez, A.C., Cheng, M.H., Schurdak, M.E., Liu, B., Chan, S.Y., Arumugaswami, V., Stern, A.M., Taylor, D.L., Arditi, M., Bahar, I., 2021. A systems-level study reveals host-targeted repurposable drugs against SARS-CoV-2 infection. Mol. Syst. Biol. 17, e10239.
Contreras, X., Mzoughi, O., Gaston, F., Peterlin, M.B., Bahraoui, E., 2012. Protein kinase C-delta regulates HIV-1 replication at an early post-entry step in macrophages. Retrovirology 9, 37.
Cortese, M., Goellner, S., Acosta, E.G., Neufeldt, C.J., Oleksiuk, O., Lampe, M., Haselmann, U., Funaya, C., Schieber, N., Ronchi, P., Schorb, M., Pruunsild, P., Schwab, Y., Chatel-Chaix, L., Ruggieri, A., Bartenschlager, R., 2017. Ultrastructural characterization of Zika virus replication factories. Cell Rep. 18, 2113–2123.
Daikonya, A., Katsuki, S., Wu, J.B., Kitanaka, S., 2002. Anti-allergic agents from natural sources (4): anti-allergic activity of new phloroglucinol derivatives from Mallotus philippensis (Euphorbiaceae). Chem. Pharm. Bull. (Tokyo) 50, 1566–1569.
Filone, C.M., Hanna, S.L., Caino, M.C., Bambina, S., Doms, R.W., Cherry, S., 2010. Rift valley fever virus infection of human cells and insect hosts is promoted by protein kinase C epsilon. PLoS One 5, e15483.
Grant, A., Ponia, S.S., Tripathi, S., Balasubramaniam, V., Miorin, L., Sourisseau, M., Schwarz, M.C., Sanchez-Seco, M.P., Evans, M.J., Best, S.M., Garcia-Sastre, A., 2016. Zika virus targets human STAT2 to inhibit type I interferon signaling. Cell Host Microbe 19, 882–890.
Hamel, R., Dejarnac, O., Wichit, S., Ekchariyawat, P., Neyret, A., Luplertlop, N., Perera-Lecoin, M., Surasombatpattana, P., Talignani, L., Thomas, F., Cao-Lormeau, V.M., Choumet, V., Briant, L., Despres, P., Amara, A., Yssel, H., Misse, D., 2015. Biology of Zika virus infection in human skin cells. J. Virol. 89, 8880–8896.
Ietta, F., Maioli, E., Daveri, E., Gonzaga Oliveira, J., da Silva, R.J., Romagnoli, R., Cresti, L., Maria Avanzati, A., Paulesu, L., Barbosa, B.F., Gomes, A.O., Roberto Mineo, J., Ferro, E.A.V., 2017. Rottlerin-mediated inhibition of Toxoplasma gondii growth in BeWo trophoblast-like cells. Sci. Rep. 7, 1279.
Ishii, R., Horie, M., Saito, K., Arisawa, M., Kitanaka, S., 2002. Prostaglandin E(2) production and induction of prostaglandin endoperoxide synthase-2 is inhibited in a murine macrophage-like cell line, RAW 264.7, by Mallotus japonicus phloroglucinol derivatives. Biochim. Biophys. Acta 1571, 115–123.
Kang, Y.L., Oh, C., Ahn, S.H., Choi, J.C., Choi, H.Y., Lee, S.W., Choi, I.S., Song, C.S., Lee, J.B., Park, S.Y., 2021. Inhibition of endocytosis of porcine reproductive and respiratory syndrome virus by rottlerin and its potential prophylactic administration in piglets. Antivir. Res. 195, 105191.
Kuno, G., Chang, G.J., 2007. Full-length sequencing and genomic characterization of Bagaza, Kedougou, and Zika viruses. Arch. Virol. 152, 687–696.
Lama, Z., Gaudin, Y., Blondel, D., Lagaudriere-Gesbert, C., 2019. Kinase inhibitors tyrphostin 9 and rottlerin block early steps of rabies virus cycle. Antivir. Res. 168, 51–60.
Lazear, H.M., Diamond, M.S., 2016. Zika virus: new clinical syndromes and its emergence in the western hemisphere. J. Virol. 90, 4864–4875.
Maioli, E., Greci, L., Soucek, K., Hyzdalova, M., Pecorelli, A., Fortino, V., Valacchi, G., 2009. Rottlerin inhibits ROS formation and prevents NFkappaB activation in MCF-7 and HT-29 cells. J. Biomed. Biotechnol. 2009, 742936.
Maioli, E., Torricelli, C., Valacchi, G., 2012. Rottlerin and cancer: novel evidence and mechanisms. Sci. World J. 2012, 350826.
Mori, N., Ishikawa, C., Senba, M., 2015. Activation of PKC-delta in HTLV-1-infected T cells. Int. J. Oncol. 46, 1609–1618.
Mukhopadhyay, S., Kuhn, R.J., Rossmann, M.G., 2005. A structural perspective of the flavivirus life cycle. Nat. Rev. Microbiol. 3, 13–22.
Musso, D., Gubler, D.J., 2016. Zika virus. Clin. Microbiol. Rev. 29, 487–524.
Oehler, E., Watrin, L., Larre, P., Leparc-Goffart, I., Lastere, S., Valour, F., Baudouin, L., Mallet, H., Musso, D., Ghawche, F., 2014. Zika virus infection complicated by Guillain-Barre syndrome–case report, French Polynesia, December 2013. Euro Surveill. 19, 20720.
Ojha, D., Winkler, C.W., Leung, J.M., Woods, T.A., Chen, C.Z., Nair, V., Taylor, K., Yeh, C.D., Tawa, G.J., Larson, C.L., Zheng, W., Haigh, C.L., Peterson, K.E., 2021a. Rottlerin inhibits La Crosse virus-induced encephalitis in mice and blocks release of replicating virus from the Golgi body in neurons. Nat Microbiol 6, 1398–1409.
Ojha, D., Woods, T.A., Peterson, K.E., 2021b. Drug-screening strategies for inhibition of virus-induced neuronal cell death. Viruses 13, 2317.
Oliphant, T., Engle, M., Nybakken, G.E., Doane, C., Johnson, S., Huang, L., Gorlatov, S., Mehlhop, E., Marri, A., Chung, K.M., Ebel, G.D., Kramer, L.D., Fremont, D.H., Diamond, M.S., 2005. Development of a humanized monoclonal antibody with therapeutic potential against West Nile virus. Nat. Med. 11, 522–530.
Pandey, S., Chatterjee, A., Jaiswal, S., Kumar, S., Ramachandran, R., Srivastava, K.K., 2016. Protein kinase C-delta inhibitor, Rottlerin inhibits growth and survival of mycobacteria exclusively through Shikimate kinase. Biochem. Biophys. Res. Commun. 478, 721–726.
Pierson, T.C., Diamond, M.S., 2018. The emergence of Zika virus and its new clinical syndromes. Nature 560, 573–581.
Pierson, T.C., Graham, B.S., 2016. Zika virus: immunity and vaccine development. Cell 167, 625–631.

Raghu, H., Sharma-Walia, N., Veettil, M.V., Sadagopan, S., Chandran, B., 2009. Kaposi's sarcoma-associated herpesvirus utilizes an actin polymerization-dependent macropinocytic pathway to enter human dermal microvascular endothelial and human umbilical vein endothelial cells. J. Virol. 83, 4895–4911.

Sandgren, K.J., Wilkinson, J., Miranda-Saksena, M., McInerney, G.M., Byth-Wilson, K., Robinson, P.J., Cunningham, A.L., 2010. A differential role for macropinocytosis in mediating entry of the two forms of vaccinia virus into dendritic cells. PLoS Pathog. 6, e1000866.

Schuler-Faccini, L., Ribeiro, E.M., Feitosa, I.M., Horovitz, D.D., Cavalcanti, D.P., Pessoa, A., Doriqui, M.J., Neri, J.I., Neto, J.M., Wanderley, H.Y., Cernach, M., El-Husny, A.S., Pone, M.V., Serao, C.L., Sanseverino, M.T., 2015. Brazilian medical genetics society-zika embryopathy task, F., 2016. Possible association between Zika virus infection and microcephaly - Brazil. MMWR Morb. Mortal. Wkly. Rep. 65, 59–62.

Shivshankar, P., Lei, L., Wang, J., Zhong, G., 2008. Rottlerin inhibits chlamydial intracellular growth and blocks chlamydial acquisition of sphingolipids from host cells. Appl. Environ. Microbiol. 74, 1243–1249.

Stiasny, K., Fritz, R., Pangerl, K., Heinz, F.X., 2011. Molecular mechanisms of flavivirus membrane fusion. Amino Acids 41, 1159–1163.

Tapia, J.A., Jensen, R.T., Garcia-Marin, L.J., 2006. Rottlerin inhibits stimulated enzymatic secretion and several intracellular signaling transduction pathways in pancreatic acinar cells by a non-PKC-delta-dependent mechanism. Biochim. Biophys. Acta 1763, 25–38.

Torricelli, C., Fortino, V., Capurro, E., Valacchi, G., Pacini, A., Muscettola, M., Soucek, K., Maioli, E., 2008. Rottlerin inhibits the nuclear factor kappaB/cyclin-D1 cascade in MCF-7 breast cancer cells. Life Sci. 82, 638–643.

Tsetsarkin, K.A., Kenney, H., Chen, R., Liu, G., Manukyan, H., Whitehead, S.S., Laassri, M., Chumakov, K., Pletnev, A.G., 2016. A full-length infectious cDNA clone of Zika virus from the 2015 epidemic in Brazil as a genetic platform for studies of virus-host interactions and vaccine development. mBio 7, e01114–e01116.

Valacchi, G., Pecorelli, A., Sticozzi, C., Torricelli, C., Muscettola, M., Aldinucci, C., Maioli, E., 2011. Rottlerin exhibits antiangiogenic effects in vitro. Chem. Biol. Drug Des. 77, 460–470.

Wang, B., Thurmond, S., Hai, R., Song, J., 2018. Structure and function of Zika virus NS5 protein: perspectives for drug design. Cell. Mol. Life Sci. 75, 1723–1736.

Yu, Y., Deng, Y.Q., Zou, P., Wang, Q., Dai, Y., Yu, F., Du, L., Zhang, N.N., Tian, M., Hao, J.N., Meng, Y., Li, Y., Zhou, X., Fuk-Woo Chan, J., Yuen, K.Y., Qin, C.F., Jiang, S., Lu, L., 2017. A peptide-based viral inactivator inhibits Zika virus infection in pregnant mice and fetuses. Nat. Commun. 8, 15672.

Zheng, F., Li, N., Xu, Y., Zhou, Y., Li, Y.P., 2021. Adaptive mutations promote hepatitis C virus assembly by accelerating core translocation to the endoplasmic reticulum. J. Biol. Chem. 296, 100018.

Zhou, S., Yang, C., Zhao, F., Huang, Y., Lin, Y., Huang, C., Ma, X., Du, J., Wang, Y., Long, G., He, J., Liu, C., Zhang, P., 2019. Double-stranded RNA deaminase ADAR1 promotes the Zika virus replication by inhibiting the activation of protein kinase PKR. J. Biol. Chem. 294, 18168–18180.